

Experiments on the Structure of an Individual Elementary Particle

HANS DEHMELT

Research begun in the early 1970s on geonium is reviewed. Geonium is a man-made atom, created at liquid-helium temperature in ultrahigh vacuum from an individual electron in magnetic and electric trapping fields. For this atom the electron gyromagnetic ratio $g = 2.000\,000\,110(60)$ has been measured in microwave spectroscopy experiments after subtraction of quantum electrodynamics shifts. The $g - g_{\text{Dirac}} = 11 \times 10^{-11}$ excess over the value $g_{\text{Dirac}} = 2$ for the theoretical Dirac point electron suggests for the electron of nature a corresponding excess radius $R_e - R_{\text{Dirac}}$ over the Dirac radius $R_{\text{Dirac}} = 0$ and a spatial structure. From a plot of measured g and R values for the near-Dirac particles electron, proton, triton, and helium-3, an electron radius $R_e \approx 10^{-20}$ centimeter is extrapolated. In a speculation, the triton-proton-quark model has been extended to the electron, to a succession of subquarks, and finally to the "cosmon." Rapid decay of a cosmon-anticosmon pair created from the "nothing" state in a spontaneous quantum jump initiated the Big Bang.

"You know, it would be sufficient to really understand the electron."

Albert Einstein

STUDIES (1) OF THE STRUCTURE OF AN INDIVIDUAL ELEMENTARY particle were begun in Seattle in 1976. In these experiments an electron, almost at rest, was isolated and closely confined quasi-permanently. Changes in its quantum states were induced and continuously observed, as they occurred at random, eventually for months. In fact, on 15 September 1984, Van Dyck, Schwinger, and Dehmelt (2, 3) were able to announce: "Here, right now, in a little cylindrical domain, about 30 μm in diameter and 60 μm long, in the center of our Penning trap (4) resides positron (or anti-electron) Priscilla, who has been giving spontaneous and command performances of her quantum jump ballets for the last 3 months." There can be little doubt about the identity of Priscilla during this period, since in ultrahigh vacuum she never had the chance to trade places with a passing antimatter twin. The well-defined identity of this elementary particle is something fundamentally new, which deserves to be recognized by being given a name, just as pets are given names of persons. The Seattle experiments (1-6) are quite distinct from cloud chamber or multiton detector

experiments at accelerator laboratories in which tracks of past events are studied. They also laid to rest Wolfgang Pauli's assertions (3, 6)—backed by Niels Bohr—that the spin magnetic moment of the electron could never be measured on free electrons, that is, electrons not bound to a nucleus, by means of spin-dependent changes in classical orbits.

The first evidence that an elementary particle, the proton, might not be the structureless point particle predicted by the Dirac theory came from Stern's famous 1933 experiments on a beam of hydrogen molecules, based on the 1921 Stern-Gerlach effect. He found that the intrinsic magnetism of the proton (7) was almost three times as large as the value calculated by Dirac,

$$\mu_B (\text{proton}) = qh/4\pi M \quad (1)$$

a Bohr magneton, but with q and M , respectively, the charge and mass of the proton (h is Planck's constant). At the time it was well known that in an obviously composite particle the magnetism was closely related to its structure and size. For example, the magnetism of a hydrogen atom with a hypothetical proton spin zero, which is μ_B evaluated for an electron, has the value of $\approx 1800 \gg 1$ in magneton units reflecting the total mass of the atom. The large size and magnetism of this composite spin-1/2 particle on a nucleon scale are due to its light electron constituent, and its mass is due to the proton. Thus, in analogy, Stern in 1933, and even more so Bloch in 1940 when he measured the neutron magnetism to be not zero, the Dirac value, but roughly as large as that of the proton, might very well have speculated that the nucleons contained charged lighter constituents and distantly resembled $F = 1/2$ states of H_2^+ and D. We know today they do.

Although no atom smasher has yet succeeded in cracking the electron apart and revealing a structure in this fashion, it is far from implausible that, like Democritus's atom and Dirac's point proton before, Dirac's point electron and even its components will turn out to be composite in a never-ending regression. It is also plausible that, in analogy with the proton, the structure and radius of the electron will be reflected in its magnetism. Therefore, it is no surprise that experimental studies of the electron magnetism have attracted great interest since the experiments of Einstein and de Haas and Stern and Gerlach. Work from 1920 to 1972 is reviewed by Rich and Wesley (8).

Penning Trap and Geonium Atom

One forms the metastable pseudoatom geonium (1, 5, 6) by permanently confining an individual electron at the well bottom of an ultrahigh-vacuum Penning trap (4) (Fig. 1). The trap is related to Hull's magnetron, which I got to know well in an atomic physics

The author is in the Department of Physics, FM-15, University of Washington, Seattle, WA 98195.

Fig. 1. Penning trap. The simplest motion of an electron in the trap is along its symmetry axis, along a magnetic field line. Each time an electron comes too close to one of the negatively charged caps, it turns around. The resulting harmonic oscillation took place at about 60 Mhz in our trap. [Adapted from (9) with permission, copyright Plenum Press]

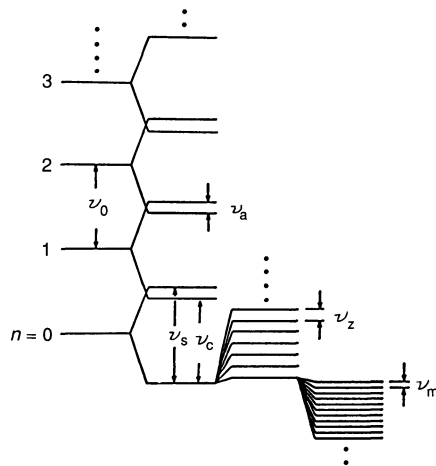
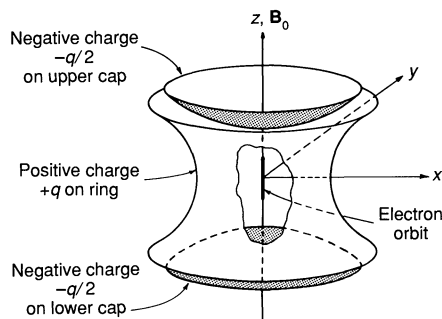


Fig. 2. Energy levels of geonium. [Adapted from (5) with permission, copyright Plenum Press]

laboratory class in 1946. In today's microwave ovens it is the component that transfers kilowatts of energy from a rotating trapped electron cloud to a cavity resonator, the oven chamber. It is also related to Lawrence's cyclotron, the progenitor of most of today's atom smashers. Most immediately it is derived from the Penning discharge tube. A Penning vacuum gauge first piqued my curiosity in 1952 in the glassblower's shop at Kopfermann's Institute. It occurred to me then that in a highly evacuated Penning discharge tube with an applied dc voltage of just a few volts an electron cloud might persist, even in the absence of a discharge.

Later experiments (3, 4, 9) demonstrated confinement times of a few seconds in 1959 in a sealed-off vacuum tube approximating the electrode shape of Fig. 1 and using a <50-G field. I named the device first "magnetron trap" and later "Penning trap" (4). In the current Seattle experiments this trap is constructed from a homogeneous magnetic field $B_0 = 5 \text{ T}$ and a weak electric quadrupole field

$$\Phi(xyz) = A(x^2 + y^2 - 2z^2) \quad (2)$$

which provides an axial potential well of depth

$$D = e[\Phi(000) - \Phi(00Z_0)] = 2eAZ_0^2 = 5 \text{ eV} \quad (3)$$

where e is the electron charge. Cap-to-cap separation in the trap is $2Z_0 \approx 0.8 \text{ cm}$.

The energy levels of geonium (5) are shown in Fig. 2. They reflect the slightly shifted circular cyclotron motion at $\approx \nu_c = eB_0/2\pi m_e = 141 \text{ GHz}$ (m_e is the electron mass), the spin precession at $\nu_s \approx \nu_c$, the anomaly or $g - 2$ frequency $\nu_a = \nu_s - \nu_c = 164 \text{ MHz}$, the axial oscillation at $\nu_z = 64 \text{ MHz}$, and the circular magnetron or drift motion at frequency $\nu_m = 14.5 \text{ kHz}$. The metastability of geonium is due to the radial potential hill provided by the electric field, which causes the magnetron motion levels to extend outward until the corresponding radius of the motion exceeds that of the ring

electrode, and the electron collides with it and is lost.

One can monitor the geonium atom continuously by exciting the ν_z oscillation and detecting with a shortwave radio receiver the stimulated emission at $\approx 60 \text{ MHz}$, which is enhanced 10^9 -fold by coupling the electron to an inductance/capacitance (LC) resonator. Transitions at the frequencies ν_c , ν_a , and ν_m are observed by means of the continuous Stern-Gerlach effect described below, which slightly shifts the frequency of the monitored ν_z signal and thereby signals the occurrence of jumps (1) in the respective quantum number.

Electron-Resonant Circuit Interaction

For the purpose of continuously detecting the trapped electron and, at the same time, cooling its axial motion after injection, a resonant circuit tuned to the electron frequency $\nu_z \approx 60 \text{ MHz}$ is connected between the cap electrodes. The electron-circuit interaction (Fig. 3) was analyzed (9) for arbitrary charge e and mass M in 1962, by approximating the hyperbolic cap electrodes by plane capacitor plates spaced $2Z_0$ apart. An otherwise undamped electron oscillation of initial energy W_1 excites the resonant circuit to a coherent oscillation of very small energy $W_T \ll W_1$. In spite of rapid loss due to the presence of the shunt resistance R_S , W_T only decreases slowly. Its magnitude is determined by the requirement that the energy loss into R_S , with the characteristic time constant $\tau_{TB} = R_S C$, be balanced by energy input from the oscillating electron. With τ_{IT} the time constant for energy transfer from electron to the LC circuit, we may write accordingly

$$W_1/\tau_{IT} = W_T/\tau_{TB} \quad (4)$$

The mechanism for the energy transfer is the force exerted on the moving electron by the electric radio-frequency (rf) field between the capacitor plates that is associated with the circuit energy W_T . Analysis of this mechanism yields

$$\tau_{IT} = 4m_e Z_0^2 e^2 R_S \quad (5)$$

for the damping time of the axial electron oscillation. For R_S and the LC circuit at the bath temperature T_0 an initially higher or lower electron energy will approach kT_0 with this time constant, which in the geonium experiments had the quite small value $\tau_{IT} \approx 0.02 \text{ s}$, while $\tau_{TB} \approx 2 \mu\text{s}$.

As a simple, not necessarily very practical, way of detecting the presence of the electron, one might think of pulling it toward one of the caps by slowly applying a dc field between them, which then is

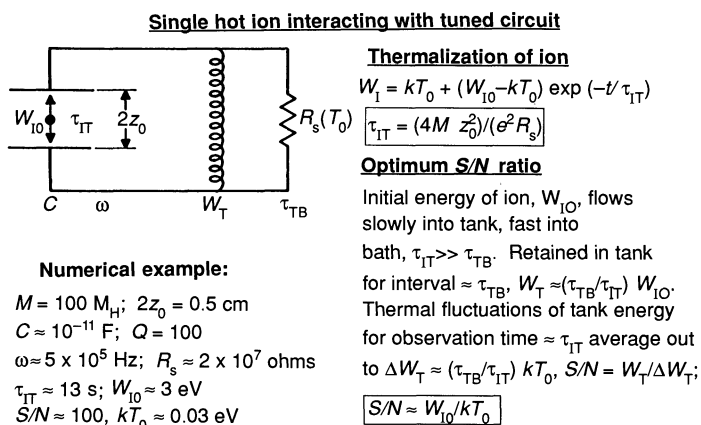


Fig. 3. An individual energetic ion interacting with a resonant LC circuit induces a signal in the circuit and is damped and cooled by the interaction. [Adapted from (9) with permission, copyright Plenum Press]

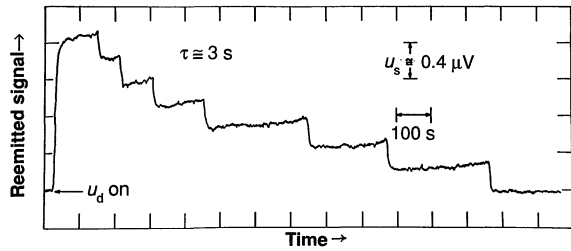


Fig. 4. Radio-frequency signal produced by trapped electron. When the electron is driven by an axial rf field, it emits a 60-MHz signal, which was picked up by a radio receiver. The signal shown was for a very strong drive (u_d) and an initially injected bunch of seven electrons. One electron after the other was randomly “boiled” out of the trap until finally only a single one was left. By somewhat reducing the drive, this last electron could be observed indefinitely. [Adapted from (10) with permission, copyright American Institute of Physics]

suddenly turned off, leaving the electron at rest with an initial potential energy W_{I0} . For good detectability of the electron “signal” $S = W_T$, this signal must exceed the thermal “noise” energy of the LC oscillator, $N = kT_0 \approx 350 \mu\text{eV}$ at 4 K, by a comfortable margin. However, to even realize a signal-to-noise ratio (S/N) = 1 according to Eq. 4 with these parameters, it would be necessary to excite the electron to $W_I = 3.5 \text{ eV}$ in a well only 5 eV deep. The practical solution here lies in reducing the observation band width. Although the electron signal is practically monochromatic, the noise signal is spread out over the full width $1/2\pi\tau_{TB}$ of the LC circuit resonance curve, which was about 80 kHz. Thus, if the signals are sent through a filter with a Lorentzian pass band made arbitrarily equal to $1/2\pi\tau_{IT} \approx 8 \text{ Hz}$, S will be only moderately reduced while N is cut down by a factor $\approx \tau_{TB}/\tau_{IT} \approx 10^{-4}$ so that

$$S/N \approx (W_T/kT_0) (\tau_{IT}/\tau_{TB}) = W_{I0}/kT_0 \quad (6)$$

The price for this huge increase in S/N is an equally huge increase in the time, from 2 μs to 0.02 s, needed for observing the electron signal with only moderate degradation. Equation 6 still holds, when the electron oscillation is continuously driven (10) (Fig. 4).

Side-Band Cooling

Centering the electron in the z direction, by coupling a resonant circuit to it and thereby cooling the axial oscillation, works fine, and the high-frequency cyclotron motion, even in free space, decays spontaneously in $\approx 0.1 \text{ s}$. However, splitting the ring electrode by a cut coincident with, say, the yz plane and connecting the halves by a resonant circuit tuned to ν_m would achieve the opposite for the magnetron motion. As energy is transferred to the circuit from the metastable magnetron motion, its energy would decline and its radius would grow faster and faster as the resonant circuit is excited in a maser-like fashion until the electron hits the ring electrode and is lost. This process is very similar to the one used in the microwave magnetron.

Accordingly, after injection, radial centering of the electron in the trap was far from spontaneous but required special ingenuity. Centering was achieved by rf side-band cooling (1, 5, 11) in 1976 (Fig. 5) in the first such g measurement. This cooling process is similar to the well-known “optical pumping” (12) of closely spaced atomic sublevels, which suggested in the early work (13) on atom-like electron clouds in a Penning trap that the closely spaced vibrational levels in the trap might be repopulated and the electrons cooled by analogous techniques. It provides a good example of why the concept of the geonium atom is a very useful one.

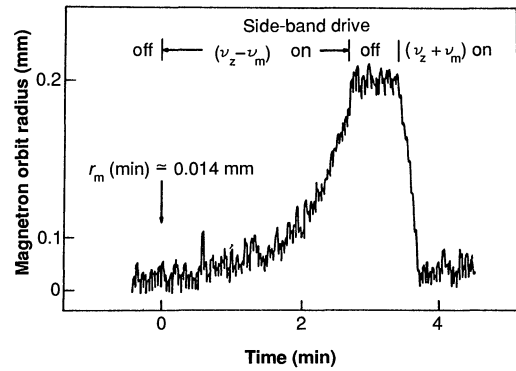
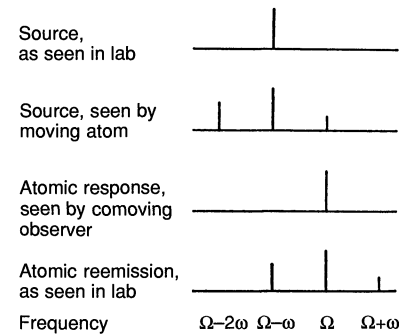


Fig. 5. Side-band “cooling” of the magnetron motion at ν_m . By driving the axial motion not on resonance at ν_z but on the lower side band at $\nu_z - \nu_m$, it is possible to force the magnetron motion to provide the energy balance $h\nu_m$ and thereby expand the magnetron orbit radius. Conversely, an axial drive at $\nu_z + \nu_m$ shrinks the radius. The roles of upper and lower side bands are reversed here from the case of a particle in a well where the energy increases with amplitude because the magnetron motion is metastable and the energy of motion decreases with radius. [Adapted from (5) with permission, copyright Plenum Press]

Fig. 6. Side-band cooling of a trapped ion by a wave tuned to lower side band. The ion oscillates in the propagation direction of the electromagnetic wave. [Adapted from (3) with permission, copyright the Royal Swedish Academy of Sciences]



As a simple model (3) I describe side-band cooling of a trapped ion restricted to move in a straight line (Fig. 6). The ion is irradiated by a monochromatic plane electromagnetic wave of frequency $\Omega - \omega$. Because of the Doppler effect, the source signal seen by the ion is frequency-modulated at $\omega \ll \Omega$ since the velocity of the ion oscillating in the trap at ω varies periodically at the same frequency. Therefore, the source spectrum shows two (or more) side bands (9, 13) spaced at ω symmetrically around $\Omega - \omega$. This tuning of the source makes its upper side band coincide with an internal resonance at frequency Ω of the ion and excites the ion. The signal reemitted by the ion is again split by the Doppler effect but has an average frequency of $\approx \Omega$. In this process a source photon of energy $\hbar(\Omega - \omega)$ is transformed into a reemitted one of average energy $\approx \hbar\Omega$ by borrowing $\hbar\omega$ from the oscillatory motion, which is thereby cooled.

Side-band cooling by a standing $(\Omega - \omega)$ wave (14), which is equivalent to two waves traveling in opposite directions, may be analyzed in a similar fashion. With an electric field node at the ion site, it has the advantages of minimal excitation of the ion. In side-band cooling of the magnetron motion in geonium, the inhomogeneous rf field at $\nu_{zd} = \nu_z \pm \nu_m$ used here can be viewed as a part of a standing wave. Figure 5 shows the heating and cooling effects observed when the excitation frequency ν_{zd} is first tuned to $\nu_z - \nu_m$ and then to $\nu_z + \nu_m$. This 1977 demonstration (5) of side-band cooling based on rf excitation raises the question of how small a magnetron radius can be realized in this way. For a model, in which both the z motion to be cooled and the y motion used for cooling are classical harmonic oscillations at ω and Ω , respectively, a simple classical treatment based on radiation pressure pulsing at ω solves

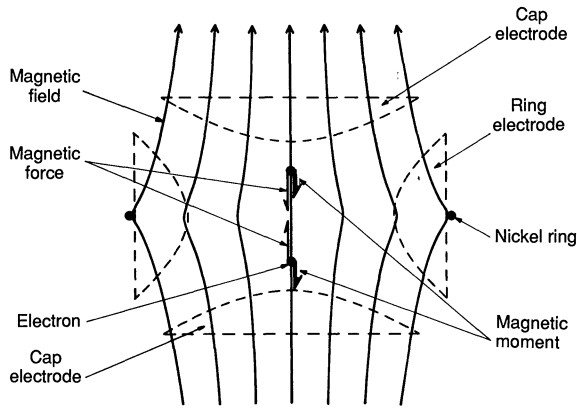


Fig. 7. Weak magnetic bottle for continuous Stern-Gerlach effect. The electron forms a wave packet that is $1 \mu\text{m}$ long and 30 nm in diameter, which oscillates undistorted in the axial electric potential well. The inhomogeneous field of the auxiliary magnetic bottle produces a minute spin-dependent restoring force that causes the axial frequency ν_z for spin \uparrow and \downarrow to differ by a small but detectable value. [Adapted from (17) with permission, copyright Springer-Verlag]

this problem (15). The result is most succinctly expressed in quantum-mechanical terms,

$$\langle n \rangle \approx \langle N \rangle \quad (7)$$

where $\langle N \rangle$ is the average quantum level for the γ motion, thermally excited at the temperature T_0 , and $\langle n \rangle$ is the lowest average quantum level of z -motion excitation that the side-band cooling can produce in the absence of any external heating.

Continuous Stern-Gerlach Effect

Unlike at the axial frequency ν_z , the direct detection of absorption or emission of quanta by the geonium atom at cyclotron, anomaly, and magnetron frequencies is not feasible. Detection of transitions at these frequencies is made possible by the continuous Stern-Gerlach effect (16, 17) invented in 1973. Like the classic beam deflection effect, it relies on a change in the magnetic moment of a quantum state. It signals a transition between two states by a shift of the axial frequency proportional to the accompanying change in magnetic moment.

The shallow magnetic bottle or Lawrence trap used for the continuous Stern-Gerlach effect (Fig. 7) was in the first experiments (1, 5) produced by two turns of 5-mil nickel wire wound around the

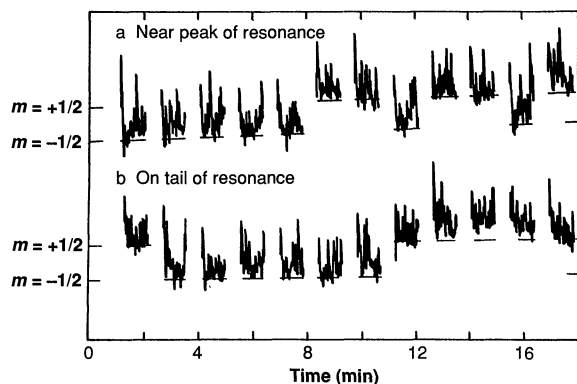


Fig. 8. Jumps in the spin quantum number m for tuning of the excitation (a) on the spin resonance and (b) on the tail of the resonance. [Adapted from (2) with permission, copyright World Scientific Publishing]

Fig. 9. Phase-sensitive detection circuit for the axial resonance at ν_z . The elastically bound electron oscillator acts effectively like an LC resonant circuit oscillator; Atten., attenuator; A, amplifier. [Adapted from (5) with permission, copyright Plenum Press]

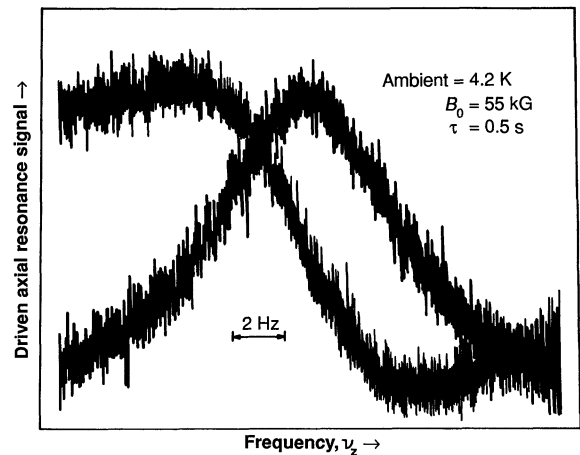
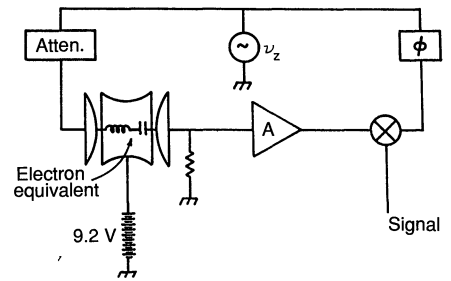


Fig. 10. Plots of driven axial resonance amplitudes versus electron eigen frequency ν_z . The latter is slowly swept by varying the depth of the confining potential well. The graph shows the absorption mode and also the S-shaped dispersion mode, for which the zero is raised. Note the about one part in 10^7 width of the resonance. [Adapted from (5) with permission, copyright Plenum Press]

ring electrode. The large applied magnetic field \mathbf{B}_0 magnetized the wire to saturation and produced a bottle field \mathbf{b} , practically independent of B_0 . Near the origin, the trap center, its z component was, with $\beta = 120 \text{ T/m}^2$,

$$b_z = \beta(z^2 - r^2/2) \quad (8)$$

and added to \mathbf{B}_0 . The effectiveness of this scheme was first tested by exciting the cyclotron motion, which requires very little millimeter wave power, and watching for a shift in the axial frequency ν_z . The quantized energy of the cyclotron motion is given by

$$E_n = (n + 1/2)h\nu_c \quad (9)$$

By setting

$$-\mu_n B_0 = E_n \quad (10)$$

one can assign a quantized magnetic moment $\mu_n = -(2n + 1)\mu_B$ to the n th cyclotron level. This magnetic moment interacts with the magnetic bottle (Fig. 7). On the z axis the difference of the potential energy of the electron at $z = Z_0$ and $z = 0$, or the total depth D of the axial confining well, is then given by

$$D = D_e + D_m, \quad D_m = (2n + 1)\mu_B \beta Z_0^2 \quad (11)$$

where $D_e = 5 \text{ eV}$ is the electrostatic part of the well depth, and $D_m \approx 0.2(n + 1/2) \mu\text{eV}$ is the magnetic "Stern-Gerlach" contribution. Since for a confining well with fixed Z_0 the relation between oscillation frequency, force constant, and depth is $\nu_z^2 \propto k \propto D$, and $D_m \ll D_e$, we have for the shift associated with the n th cyclotron state

$$\delta\nu_z \approx 1/2(D_m/D_e)\nu_z = (n + 1/2)\delta$$

$$\delta = \mu_B\beta/2\pi^2m_e\nu_z \approx 1 \text{ Hz} \quad (12)$$

with $\mu_B = eh/4\pi m_e$, the Bohr magneton. We were able to see even the excitation by the thermal radiation field. Examining Fig. 8, for which $\langle n \rangle \approx 0.23$ at 4 K, one recognizes frequent intervals of an average length of about 5 s for which $m = -1/2$, $n = 0$ (m , spin quantum number; n , cyclotron quantum number). This shows that for the spin and also at least for one degree of freedom of the translational electron motion the zero-point energy is frequently attained.

Recognizing that spin and magnetron motions are associated with quantized magnetic moments $\mu_m = 2m\mu_B$, $\mu_q \approx 2q(\nu_m/\nu_c)\mu_B$, with m and q the spin and magnetron quantum numbers, we may extend Eq. 12 to

$$\delta\nu_z \approx [m + n + 1/2 + (\nu_m/\nu_c)q]\delta \quad (13)$$

The weak q dependence was sufficient for the demonstration of side-band cooling in Fig. 5.

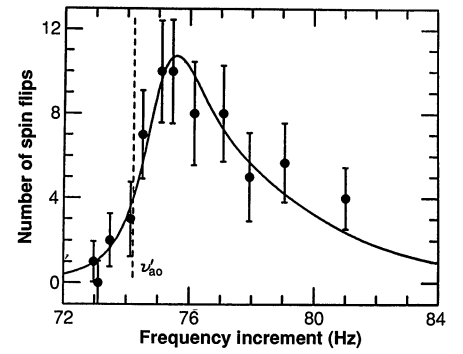
The measurement of the frequency shift $\delta\nu_z$ to fractions of 1 Hz out of 60 MHz obviously required a bit of effort (5). The narrow filter introduced above is realized by a phase-sensitive detector (10) (Fig. 9). It has a low-pass, resistance/capacitance (RC) filter (not shown) in the output line, which averages out the higher frequency components in the detected noise signal. By adjusting the phase ϕ of the reference signal in this circuit, one may obtain the dispersion signal of Fig. 10, for which the zero-response level has been raised in the graph. One sees that the signal vanishes on exact resonance and near zero decreases linearly with frequency. Obviously, this signal could serve to detect a small frequency shift of 1 Hz in the axial resonance with good S/N and could function as frequency shift monitor for the continuous Stern-Gerlach effect. Its analog in the classic Stern-Gerlach effect for atomic beams is the glass plate on which the beam of silver atoms was collected. Actually, in the experiments (1, 5), a more complex frequency-locking scheme and side-band excitation (10) as well as a compensated trap (2, 9, 16) were used.

Spin and Cyclotron Resonances

The most straightforward approach to measuring the spin precession frequency ν_s would seem to be as follows. Induce up and down jumps between the two spin states $m = -1/2$ and $+1/2$ by irradiating the electron with a millimeter wave whose frequency ν_{sd} is slowly stepped through the resonance at ν_s of shape $G_s(\nu)$. Remaining at each step for the same time interval, by constantly monitoring the axial frequency ν_z , count (1) the number of random jumps (Fig. 8) in the time interval by means of the continuous Stern-Gerlach effect, which should be proportional to $G_s(\nu)$. Alas, this straightforward approach is far from optimal when $\nu_s \approx \nu_c$ and one is chiefly interested in the small frequency difference between these two equally broadened resonances. By allowing one to subtract this broadening in measuring $\nu_a = \nu_s - \nu_c$ directly (1, 5), side-band excitation (10, 13) can make another decisive contribution. The electron, when moving at the cyclotron frequency ν_c through an inhomogeneous magnetic rf field at ν_{ad} , "sees" in its rest frame also side bands at $|\nu_{ad} \pm \nu_c|$. Thus, by choosing $\nu_{ad} + \nu_c = \nu_s$ one can tune one side band to the spin resonance and induce spin flips. Not even a millimeter wave source is required, because the cyclotron motion is excited thermally and the correct ν_{ad} value falls near 164 MHz.

However, another serious problem remains. The axial motion through the magnetic bottle field shifts ν_s and ν_c proportional to

Fig. 11. Electron spin resonance in geonium near 141 GHz. [Adapted from (10) with permission, copyright American Institute of Physics]



axial energy W_z . Worse, W_z contains a cross term $\propto z_t z_c$, where z_t and z_c are oscillation amplitudes excited thermally and by the coherent applied drive. This random-amplitude cross term, which grows proportional to the applied detection drive amplitude, greatly broadens the ν_s , ν_c resonances. The solution here lies in alternating (5) periods of spin-flip excitation (during which the axial detection drive is turned off) with monitoring periods (in which the axial drive necessary for ν_z measurement is on but the spin-flip excitation is off). Now for very strong spin resonance excitation the probabilities of finding spin up or down in a monitoring period are 50% each, and, on the average, in N excitation-monitoring cycles one can count no more than $N/2$ random jumps between the two levels. This indicates saturation of the resonance and strong distortion of the weak-signal line shape one is looking for. In the resonance shown in Fig. 11 a reasonable compromise was struck with a maximum count of 10 jumps in 25 cycles. The cyclotron resonance was obtained in a similar alternating fashion (2).

In the energy level diagram of Fig. 2 a spin flip $\Delta n = 0$, $m = -1/2 \rightarrow +1/2$ induced in the above fashion may be viewed as a transition $n = 0 \rightarrow 1$ due to thermal radiation followed by a transition ($n = 1$, $m = -1/2$) \rightarrow ($n = 0$, $m = +1/2$) induced by the applied rf field at ν_a .

Electron g Factor and Size

In the analysis of atomic spectra the dimensionless gyromagnetic ratio or g factor (18) $g = \mu/J$, with μ , J in units μ_B (Eq. 1) and \hbar , respectively, has been introduced for an atomic state with magnetic moment μ and angular momentum J . In ordinary units this boils down to

$$g = (\mu/J)/(2M/q) \quad (14)$$

with q and M being, respectively, the charge and mass of the electron. In the case of particles originally perceived as noncomposite the concept has been adapted by redefining q and M as total charge and mass of the particle, which yields for the proton $g = 5.6$, for example. Rewriting Eq. 14 as

$$g = 2(\mu_B q / 2\pi J) / (q B_0 / 2\pi M) = 2\nu_s / \nu_c \quad (15)$$

we see that g may conveniently be obtained by measuring spin and cyclotron frequencies in the same constant field B_0 . In this way the gyromagnetic ratios $g = 2\nu_s / \nu_c = 2(1 + \nu_a / \nu_c)$ for electron and positron were eventually measured (19) in 1987 with an estimated error of 4 parts in 10^{12} ,

$$g/2 = \nu_s / \nu_c = 1.001\,159\,652\,188(4) \quad (16)$$

The ratio $g(e^+)/g(e^-) = 1 + (0.5 \pm 2) \times 10^{-12}$ found yields the most stringent test of charge-parity-time (CPT) reversal or matter-antimatter symmetry for charged particles. For the Dirac point

small size of these two very short-lived particles makes possible their tight binding, which in an extreme extension of the Fermi-Yang idea preserves the required zero total relativistic energy or mass of the bound pair or "cosmonium atom." The subsequent explosion of cosmonium into more and more ever lighter but more complex decay products, wider and wider dispersed, then forms the early hot universe envisioned in the standard Big Bang. However, no infinitely small point particles or singularities appear in our picture of a universe finite in the large and small. The cosmonium atom introduced here is merely an updated version of Georges Lemaître's "l'atome primitif," the world atom, whose explosion into the primordial fireball he discussed in his 1950 book (26a).

Conclusions

The study of geonium has resulted in an improvement of three or more orders of magnitude in the accuracy attained in magnetic moment measurements for elementary particles. The principal result, a value of the electron gyromagnetic ratio exceeding Dirac's value 2 by 11×10^{-11} , suggests an electron radius $R_e \approx 10^{-20}$ cm and contributes to a better understanding of the composite structure of the electron, its subquark components, and the Big Bang. Also, with the growing extension of techniques demonstrated in geonium work to the mass spectroscopy (3, 27, 28) of single atomic matter and antimatter ions, to the optical region (3, 29-31) [although no attempt has been made in Seattle to photograph Priscilla, blue barium ion Astrid (3, 32) has been photographed in color and visually observed in similar experiments], to photon statistics (33), ion crystal (34, 35), and chaos (36) studies, and to neutral atoms (37, 38), a discussion of the ideas underlying the geonium techniques may be of use to a widening circle of readers.

REFERENCES AND NOTES

1. R. S. Van Dyck, Jr., P. Ekstrom, H. Dehmelt, *Nature* **262**, 776 (1976).
2. R. S. Van Dyck, Jr., P. Schwinberg, H. Dehmelt, in *Atomic Physics*, R. S. Van Dyck, Jr., and E. N. Fortson, Eds. (World Scientific, Singapore, 1984), vol. 9, pp. 53-74.
3. H. Dehmelt, *Phys. Scr.* **T22**, 102 (1988).
4. ———, *Adv. At. Mol. Phys.* **3**, 55 (1967); *ibid.* **5**, 109 (1969).
5. R. S. Van Dyck, Jr., P. Schwinberg, H. Dehmelt, in *New Frontiers in High Energy Physics*, B. Kursunoglu, A. Perlmutter, L. F. Scott, Eds. (Plenum, New York, 1978), pp. 159-181.
6. ———, *Phys. Dev. D* **34**, 722 (1986).
7. O. Stern, in *Les Prix Nobel en 1946*, M. P. A. L. Hallstrom *et al.*, Eds. (Norstedt and Söner, Stockholm, 1948), pp. 123-129.
8. A. Rich and J. C. Wesley, *Rev. Mod. Phys.* **44**, 250 (1972), and references therein. See also R. Conti, D. Newman, A. Rich, E. Sweetman, in *Precision Measurements and Fundamental Constants II*, B. Taylor and W. Philips, Eds. (National Bureau of Standards Special Publication 617, National Bureau of Standards, Gaithersburg, MD, 1984), p. 207, and references therein.
9. H. Dehmelt, in *Advances in Laser Spectroscopy*, F. T. Arecchi, F. Strumia, H. Walther, Eds. (Plenum, New York, 1983), pp. 153-187.
10. D. Wineland, P. Ekstrom, H. Dehmelt, *Phys. Rev. Lett.* **21**, 1279 (1973).
11. H. Dehmelt, *Nature* **262**, 777 (1976); D. Wineland and H. Dehmelt, *Bull. Am. Phys. Soc.* **20**, 637 (1975).
12. A. Kastler, *J. Opt. Soc. Am.* **47**, 460 (1957).
13. H. Dehmelt and F. Walls, *Phys. Rev. Lett.* **21**, 127 (1968); F. Walls, thesis, University of Washington (1970).
14. R. Van Dyck, Jr. *et al.*, *Bull. Magn. Resonance* **4**, 17 (1983).
15. H. Dehmelt, unpublished work; D. J. Wineland, *J. Appl. Phys.* **50**, 2528 (1979).
16. H. Dehmelt and P. Ekstrom, *Bull. Am. Phys. Soc.* **18**, 727 (1973).
17. H. Dehmelt, *Z. Phys. D* **10**, 127 (1988).
18. L. Pauling and S. Goudsmit, *The Structure of Line Spectra* (McGraw-Hill, New York, 1930), p. 69.
19. R. S. Van Dyck, Jr., P. Schwinberg, H. Dehmelt, *Phys. Rev. Lett.* **59**, 26 (1987).
20. T. Kinoshita, *Metrologia* **25**, 233 (1988).
21. H. Dehmelt, in *High-Energy Spin Physics*, K. J. Heller, Ed. (AIP Conference Proceedings No. 187, American Institute of Physics, New York, 1989), pp. 319-325.
22. S. J. Brodsky and S. D. Drell, *Phys. Rev. D* **22**, 2236 (1980).
23. L. Lyons, *Prog. Particle Nucl. Phys.* **10**, 227 (1983), and references therein.
24. H. Dehmelt, *Proc. Natl. Acad. Sci. U.S.A.* **86**, 8618 (1989).
25. W. Nagourney, J. Sandberg, H. Dehmelt, *Phys. Rev. Lett.* **56**, 2797 (1986).
26. A. Vilenkin, *Phys. Rev. D* **30**, 509 (1984).
- 26a. G. Lemaître, *The Primeval Atom* (Van Nostrand, New York, 1950).
27. R. Van Dyck, F. Moore, F. Farnham, P. Schwinberg, in *Frequency Standards and Metrology*, A. de Marchi, Ed. (Springer, New York, 1989), p. 349.
28. G. Gabrielse *et al.*, *Phys. Rev. Lett.* **63**, 1360 (1989).
29. After originally proposing laser spectroscopy on a single localized ion [H. Dehmelt, *Bull. Am. Phys. Soc.* **18**, 1521 (1973)], I initiated and guided to conclusion the first such experiments in Heidelberg [W. Neuhauser, M. Hohenstatt, P. Toschek, H. Dehmelt, *Phys. Rev. Lett.* **41**, 233 (1978); *Phys. Rev. A* **22**, 1137 (1980)]. This work produced the first photograph (black and white) of a (charged) atom and extended side-band cooling into the optical region.
30. W. M. Itano, J. C. Bergquist, D. J. Wineland, *Science* **237**, 612 (1987), and references therein.
31. H. Dehmelt, in *Frequency Standards and Metrology*, A. de Marchi, Ed. (Springer, New York, 1989), pp. 15 and 286.
32. W. Nagourney, *Comments At. Mol. Phys.* **21**, 321 (1988); P. Morrison and P. Morrison, *The Ring of Truth* (Random House, New York, 1987), p. 220.
33. F. Diedrich, J. Krause, G. Rempe, M. Scully, H. Walther, *IEEE J. Quantum Electron.* **24**, 1314 (1988).
34. F. Diedrich, E. Peik, J. Chen, W. Quint, H. Walther, *Phys. Rev. Lett.* **59**, 2931 (1988).
35. T. Sauter *et al.*, *Z. Phys. D* **10**, 153 (1988).
36. J. Hoffnagle, R. DeVoe, L. Reyna, R. Brewer, *Phys. Rev. Lett.* **61**, 255 (1988).
37. D. Pritchard, K. Helmerson, A. Martin, paper presented as part of the Proceedings 11th International Conference on Atomic Physics, Paris, 1988.
38. No individual neutral atom has so far been isolated and trapped, although there is great ferment in the field and many of the processes generic to trapped particles, previously described for electrons and ions (3, 4), are being rediscovered.
39. Suggestions for improvements of the manuscript by R. Mittleman, W. Nagourney, F. Palmer, P. Schwinberg, R. Van Dyck, Jr., N. Yu, and D. Dundore are gratefully acknowledged. This work was supported by the National Science Foundation. The article is based on invited papers presented at the 1989 annual joint meeting of the American Physical Society, the American Association of Physics Teachers, and the American Association for the Advancement of Science in San Francisco and at the 8th International Symposium on High Energy Spin Physics at the University of Minnesota, 1988.